Syntheses and Crystal Structures of Mn(II), Ni(II) and Cu(II) Coordination Compounds Assembled by Maleato and Dimethyl-2,2#-bipyridines

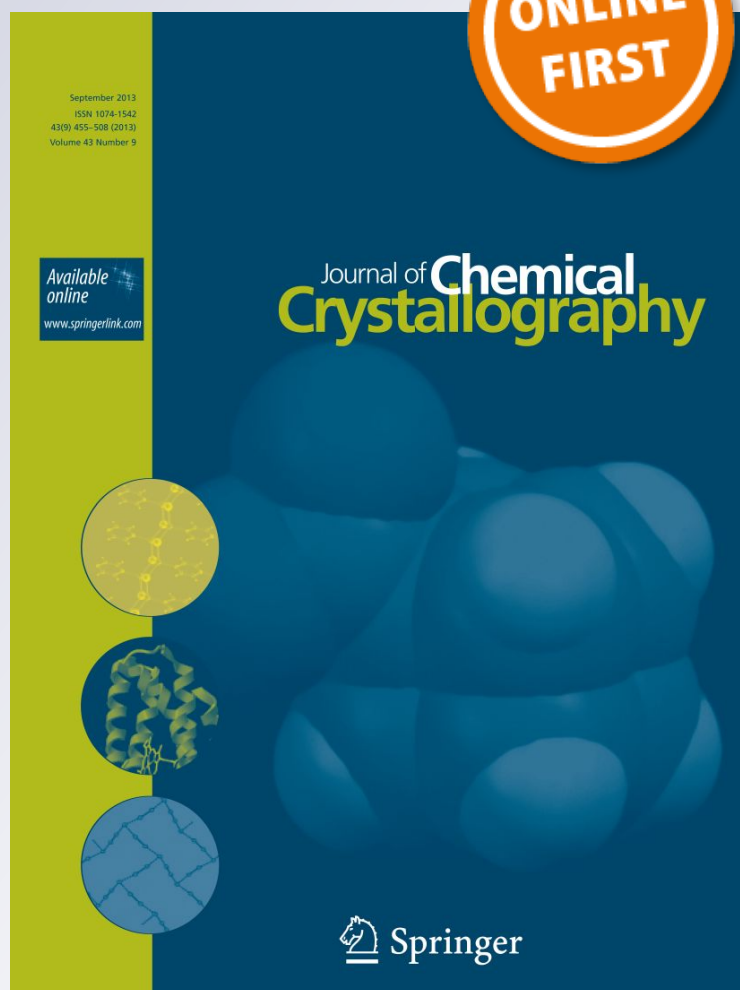## Nadia Morales-Morales, Mariana Rodríguez-Olivas, Antonio Téllez-López, Diego Martínez-Otero, Raúl A. Morales-Luckie, et al.

ONLINE FIRST

Available online
www.springerlink.com

Journal of **Chemical Crystallography**

Springer

Springer

Springer

ORIGINAL PAPER

CrossMark

Syntheses and Crystal Structures of Mn(II), Ni(II) and Cu(II) Coordination Compounds Assembled by Maleato and Dimethyl-2,2′-bipyridines

Nadia Morales-Morales[1] · Mariana Rodríguez-Olivas[1] · Antonio Téllez-López[1] · Diego Martínez-Otero[2] · Raúl A. Morales-Luckie[2] · Víctor Sánchez-Mendieta[1,2]

Abstract

Three complexes: $\{[Mn(H_2O)(mal)(5dmb)\cdot H_2O]_n\}$ (**1**); $[Ni_2(H_2O)_6(mal)_2(4dmb)_2]\cdot 3H_2O$ (**2**); $[Cu_2(mal)_2(4dmb)_2]\cdot 3H_2O$ (**3**); where mal = maleato, 4dmb = 4,4′-dimethyl-2,2′-bipyridine, and 5dmb = 5,5′-dimethyl-2,2′-bipyridine; have been synthesized, using self-assembly solution reactions at ambient conditions. Crystallographic studies show that **1** crystallizes in an orthorhombic system, space group $Pna2_1$, with $a = 17.4067(4)$ Å, $b = 11.9672(2)$ Å, $c = 8.2075(2)$ Å; $V = 1709.70(6)$ Å^3. Complex **2** has a monoclinic system, space group C2/c, with $a = 21.206(8)$ Å, $b = 7.523(3)$ Å, $c = 25.399(10)$ Å; $\beta = 109.755(8)°$; $V = 3813(2)$ Å^3. Complex **3** crystallizes in a monoclinic system, space group C2/c, with $a = 14.6976(12)$ Å, $b = 11.3849(10)$ Å, $c = 22.1638(18)$ Å; $\beta = 101.2998(17)°$; $V = 3636.8(5)$ Å^3. Complex **1** is a one-dimensional (1D) polymer, where the Mn centers are six-coordinated in a distorted octahedral geometry. **2** is a dinuclear complex, generated by supramolecular interactions, where Ni ions are six-coordinated in a distorted octahedral geometry. **3** is a dinuclear complex with five-coordinated Cu ions having a distorted square pyramidal geometry. All three complexes exhibit hydrogen bonding interactions, which generate 2D supramolecular structures in **1** and **2**, whereas in complex **3** a 3D supramolecular array is formed. These novel complexes prove that the self-assembly of a dicarboxylate ligand (mal) with three different first-row transition metals, can afford coordination compounds with diverse structural characteristics and dimensionality, which can be attributed to the different ligand coordination modes and the coordination properties of the employed metals.

✉ Víctor Sánchez-Mendieta
  vsanchezm@uaemex.mx

1 Facultad de Química, Universidad Autónoma del Estado de México, Paseo Colón y Paseo Tollocan, 50120 Toluca, Mexico State, Mexico

2 Centro Conjunto de Investigación en Química Sustentable UAEM-UNAM, Carretera Toluca-Ixtlahuaca Km. 14.5, Tlachaloya, Toluca, Mexico State, Mexico

🖄 Springer

Graphical Abstract

Divergent coordination compounds of three different transition metals have been obtained due to the versatility in the coordination modes of maleato ligand.
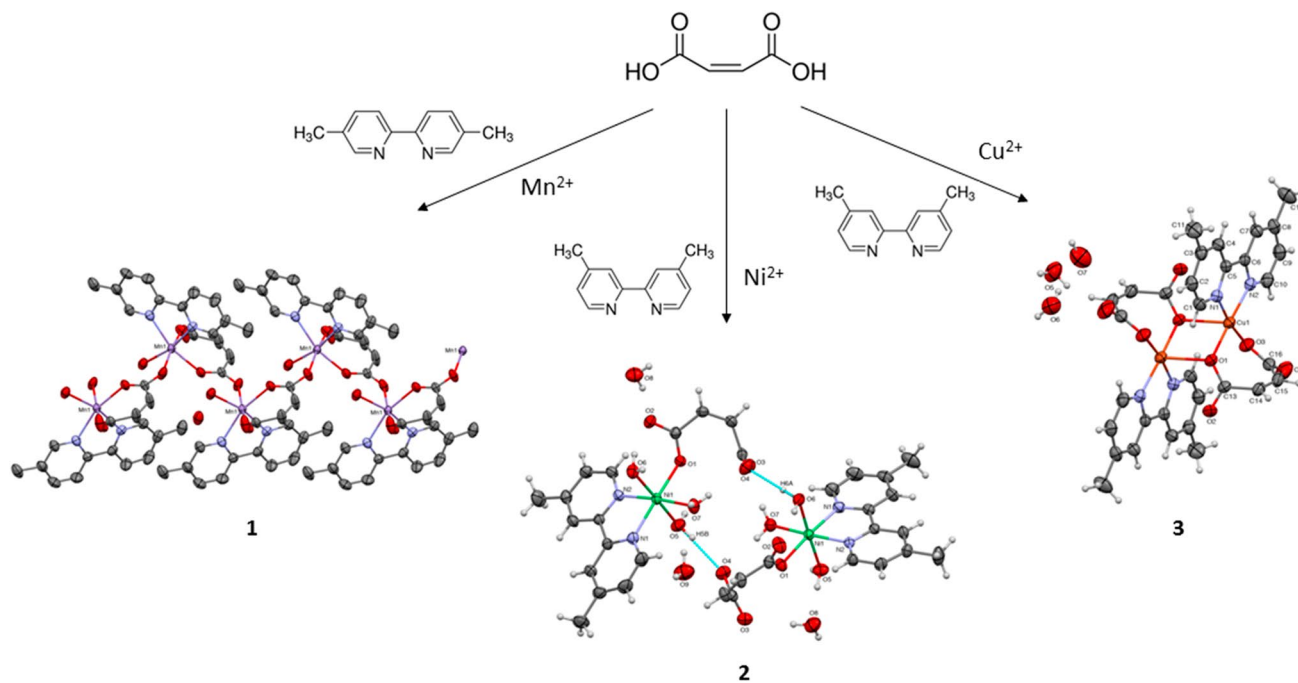
Introduction

The rational design of hybrid metal–organic polymeric and supramolecular arrays, based on crystal engineering, has gained considerable interest in recent years in coordination chemistry, supramolecular chemistry and materials science, as these structures can get fascinating arrays and can become functional materials [1]. Several strategies have been developed to synthesize metal mixed ligands coordination polymers of bivalent transition metals containing nitrogen and oxygen donor ligands [2]. One of the most used and reliable methods to generate complex compounds is the so called self-assembly. This straightforward procedure allows the preparation of both, discrete and extended coordination systems at ambient conditions. Perhaps, the only relative disadvantage of this kind of synthesis is that a precise prediction of the resultant structure can be difficult to make. This uncertainty is the result of a mixture of factors, which start with the presence of solvent molecules, type of ligands (e.g. hydrogen bonding, π–π interactions), aqua ligands, and as a consequence of the interactions of ligands and solvent molecules, mainly, supramolecular arrays come out [3]. These supramolecular arrays can influence the coordination sphere and also the final crystalline structure of the coordination

compounds; lately, supramolecular coordination arrays have been studied widely due to important properties, which can result in relevant applications such as catalysis, sensing, porosity and non-linear optics [4–6]. Carboxylates used as ion metal linkers can afford 1D, 2D or 3D polymers depending mainly on their coordination modes and, of course, on the metal ion involved [7, 8]. Therefore, in our continuing investigations on novel transition metal coordination complexes and polymers with interesting luminescent and magnetic properties [9–11], we are now involved in the generation of synthons bearing metal ions and carboxylate ligands, which eventually can function as linkers in the formation of heteronuclear coordination polymers. Maleic acid, as maleate, has been employed previously as bridging ligand in the synthesis of coordination polymers [12, 13]. Moreover, the use of bipyridine type co-ligands has long been known due to the capacity of these ligands to promote stability and crystallization of coordination complexes and polymers [14]. Up to now, few articles have been published on the use of different di-alkyl-2,2′-bipyridines as ancillary ligands, either in transition metal complexes [15] or coordination polymers [16, 17].

Herein, we describe the synthesis and crystalline molecular and supramolecular structures of three novel complexes

of Mn(II), Ni(II) and Cu(II), **1–3**, respectively, employing maleato and dimethyl-2,2′-bipyridines as ligands.

Experimental

Materials and Measurements

All chemicals were of analytical grade, purchased commercially (Aldrich) and used without further purification. All syntheses were carried out under aerobic and ambient conditions. Elemental analyses for C, H, N were obtained by standard methods using a Vario Micro-Cube analyzer. IR spectra of the complexes were determined in a FT-IR Shimadzu spectrophotometer, IR Prestige-21, from 4000 to 500 cm^{-1}.

Synthesis of 1–3

Synthesis of 1

A solution of maleic acid (0.0580 g; 0.5 mmol) in methanol (5 ml) was added to an aqueous solution (5 ml) of sodium hydroxide (0.0400 g; 1 mmol), while stirring. Then, a solution of MnCl$_2$·4H$_2$O (0.0985 g; 0.5 mmol) in deionized water (5 ml) was added, under constant stirring. Finally, a solution of 5,5′-dimethyl-2,2′-bipyridine (0.0921 g; 0.5 mmol) in methanol (5 ml) was added. A translucent yellow solution was obtained. After 3 days, the yellow crystals obtained were filtered out, washed with a 50:50 deionized water–methanol mixture and air dried. Yield: 63% based on metal precursor. Elemental analysis (%), C$_{16}$H$_{18}$MnN$_2$O$_6$, calc. C, 49.37; H, 4.66; N, 7.19; found: C, 43.54; found: C, 49.09; H, 4.60; N, 7.13. IR (cm^{-1}): 3444 (s), 3286 (s, br), 3055 (s), 2924 (m), 1682 (s, sh), 1639 (s), 1597 (vs), 1558 (vs), 1539 (vs), 1447 (s), 1439 (s), 1396 (s), 1323 (s), 1242 (s), 1165 (m), 1045 (m), 980 (m), 860 (s), 837 (s), 810 (m), 733 (m), 636 (s), 575 (m).

Synthesis of 2

A solution of 4,4′-dimethyl-2,2′-bipyridine (0.0921 g; 0.5 mmol) in methanol (5 ml) was added to a solution of maleic acid (0.0580 g; 0.5 mmol) while stirring. Then, a de-ionized water solution (10 ml) of Ni(NO$_3$)$_2$·6H$_2$O (0.1453 g; 0.5 mmol) was added. A light-blue translucent solution was obtained. After 2 days, blue crystals were achieved; these were filtered out and washed with de-ionized water. Yield: 65% based on metal precursor. Elemental analysis (%), C$_{32}$H$_{46}$N$_4$Ni$_2$O$_{17}$, calc. C, 43.87; H, 5.29; N, 6.39; found: C, 43.54; H, 5.15; N, 6.47. IR (cm^{-1}): 3410 (vs, br), 3080 (s), 2961 (m), 2921 (m), 1650 (vs, sh), 1600 (vs), 1583 (vs), 1491 (m), 1450 (m), 1410 (s), 1380 (s, sh), 1311 (m), 1289 (m), 1249 (m), 1199 (s), 1030 (m), 988 (m), 910 (m), 842 (s), 689 (w), 636 (w), 564 (w).

Synthesis of 3

A solution of maleic acid (0.0580 g; 0.5 mmol) in methanol (5 ml) was added to an aqueous solution (5 ml) of sodium hydroxide (0.0400 g; 1 mmol), while stirring. Then, a solution of Cu(NO$_3$)$_2$·2.5H$_2$O (0.1162 g; 0.5 mmol) in deionized water (5 ml) was added, under constant stirring. Finally, a solution of 4,4′-dimethyl-2,2′-bipyridine (0.0921 g; 0.5 mmol) in methanol (5 ml) was added. A translucent dark blue solution was obtained. After 5 days, the blue crystals so obtained were filtered out, washed with a 50:50 deionized water–methanol mixture and air dried. Yield: 59% based on metal precursor. Elemental analysis (%), C$_{32}$H$_{40}$Cu$_2$N$_4$O$_{14}$, calc. C, 46.20; H, 4.84; N, 6.74; found: C, 46.09; H, 4.80; N, 6.77. IR (cm^{-1}): 3406 (vs, br), 3082 (s), 2958 (s), 2920 (m), 1651 (vs, sh), 1601 (vs), 1581 (vs), 1493 (m), 1446 (s), 1412 (s), 1385 (s), 1308 (s), 1288 (m), 1246 (m), 1196 (s), 1030 (s), 987 (m), 914 (m), 910 (s), 841 (s), 683 (m), 640 (s), 598 (m), 563 (m), 521 (m).

X-Ray Crystallography

Crystallographic data for **1–3** were collected on a Bruker APEX II CCD Diffractometer, at 293 K using Mo-Kα radiation (λ = 0.71073 Å) from an Incoatec ImuS source and Helios optic monochromator [18]. Suitable crystals were coated with hydrocarbon oil (Parabar) for isolation, mounted in a glass fiber, fixed with glue and put on the goniometer head of the diffractometer for the analysis. The structures were solved using intrinsic phasing (SHELXT) [19] and refined by full-matrix least-squares on F2 [19] using the shelXle GUI [20]. The hydrogen atoms of the C–H bonds were placed in idealized positions whereas the hydrogen atoms from water molecules were localized from the difference electron density map, and their position was refined with Uiso tied to the parent atom with distance restraints. In compound **1**, the hydrogens of one methyl group present positional disorder in two positions, which was treated using the afix 123 instruction. In compound **3**, the hydrogens of water molecule, whose oxygen atoms were labeled as O6 and O7, exhibit positional disorder in two positions, the hydrogens were localized from the difference electron density map and fixed to a standard distances, the occupation were fixed to 0.5. This positional disorder establishes two different types of arrangements in the crystal by hydrogen bonds. The crystallographic data and refinement details for the complexes are summarized in Table 1. Selected bond lengths, angles and hydrogen bonding interactions for **1–3** are listed in Tables 2, 3 and 4, respectively. Chemical

Table 1 Crystal data and structure refinement parameters for **1**–**3**

	1	2	3
Empirical formula	$C_{16}H_{18}MnN_2O_6$	$C_{32}H_{46}N_4Ni_2O_{17}$	$C_{32}H_{40}Cu_2N_4O_{14}$
Formula weight	389.26	876.15	831.76
Temperature (K)	293(2)		
Wavelength (Å)	0.71073		
Crystal system	Orthorhombic	Monoclinic	
Space group	$Pna2_1$	$C2/c$	
a (Å)	17.4067(4)	21.206(8)	14.6976(12)
b (Å)	11.9672(2)	7.523(3)	11.3849(10)
c (Å)	8.2075(2)	25.399(10)	22.1638(18)
α (°)	90	90	90
β (°)	90	109.755(8)	101.2998(17)
γ (°)	90	90	90
Volume ($Å^3$)	1709.70(6)	3813(2)	3636.8(5)
Z	4	4	4
D_{calc} (mg/m^3)	1.512	1.526	1.519
Absorption coefficient (mm^{-1})	0.807	1.067	1.241
F(000)	804	1832	1720
Crystal size (mm^3)	$0.490\times0.202\times0.178$	$0.709\times0.352\times0.284$	$0.303\times0.209\times0.208$
Theta range for data collection (°)	2.340–26.355	1.704–26.367	2.280–26.334
Index ranges	$-21\leq h\leq21$, $-14\leq k\leq9$, $-10\leq l\leq10$	$-26\leq h\leq26$, $-9\leq k\leq9$, $-31\leq l\leq31$	$-18\leq h\leq18$, $-14\leq k\leq14$, $-27\leq l\leq27$
Reflections collected	16,477	18,552	17,796
Independent reflections	3470 [R(int)=0.0166]	3892 [R(int)=0.0224]	3709 [R(int)=0.0168]
Refinement method	Full-matrix least-squares on F2		
Data/restraints/parameters	3470/7/239	3892/15/279	3709/16/261
Goodness-of-fit on F2	1.057	1.057	1.052
Final R indices [I > 2sigma(I)]	R1 = 0.0186, wR2 = 0.0517	R1 = 0.0242, wR2 = 0.0644	R1 = 0.0246, wR2 = 0.0704
R indices (all data)	R1 = 0.0189, wR2 = 0.0519	R1 = 0.0262, wR2 = 0.0655	R1 = 0.0268, wR2 = 0.0718
Largest diff. peak and hole e Å^{-3}	0.175 and −0.148	0.269 and −0.234	0.250 and −0.288

structures drawings in figures were produced using Mercury software [21].

Results and Discussion

Synthesis

Using a simple methodology of self-assembling reactions, equivalent amounts of maleic acid, the corresponding metal salt, and 4,4′-dimethyl-2,2′-bipyridine and 5,5′-dimethyl-2,2′-bipyridine, respectively, were mixed in water–methanol solutions, under ambient conditions. Slow evaporation of solvents yielded single crystals of complexes **1**–**3**. It is worthwhile mentioning that the syntheses for obtaining single crystals of **1** and **3** were carried out in the same order of addition of reagents; however, for compound **2** the order of addition of the ligands to the metal salt was different, since

following the same procedure as for **1** and **3** yielded only microcrystals. NaOH was used in the syntheses of **1** and **3** for the deprotonation of maleic acid. Actually, to obtain single crystals of **2** the addition of NaOH was not required.

Crystal Structure of 1

1 Crystallizes in an orthorhombic system with a Pna2$_1$ space group and forms an infinite one dimensional (1D) coordination polymer. The repeat molecular unit of **1** contains one Mn center, one mal ligand, one 5dmb co-ligand and one coordinated water ligand. The coordination environment of Mn is shown in Fig. 1; the metal is six-coordinated and surrounded by four oxygen atoms from two different mal ligands and the aqua ligand, and two nitrogen atoms from one 5dmb ligand. The Mn has a distorted octahedral configuration. The Mn–O bond lengths range from 2.1183(15) to 2.1912(17) Å, while the Mn–N distances are 2.2847(17)

Table 2 Selected bond distances (Å), angles (°) and hydrogen bonding for **1**

Bond lengths (Å)

Mn(1)–O(4)	2.1183(15)	Mn(1)–N(2)	2.2763(18)
Mn(1)–O(2)	2.1489(16)	Mn(1)–N(1)	2.2847(17)
Mn(1)–O(3)#1	2.1523(15)		
Mn(1)–O(1)	2.1912(17)		

Angles (°)

O(4)–Mn(1)–O(2)	86.61(6)	O(3)#1–Mn(1)–N(2)	104.38(7)
O(4)–Mn(1)–O(3)#1	168.25(7)	O(1)–Mn(1)–N(2)	92.27(7)
O(2)–Mn(1)–O(3)#1	84.78(6)	O(4)–Mn(1)–N(1)	99.62(7)
O(4)–Mn(1)–O(1)	85.37(7)	O(2)–Mn(1)–N(1)	93.37(7)
O(2)–Mn(1)–O(1)	103.01(7)	O(3)#1–Mn(1)–N(1)	88.87(6)
O(3)#1–Mn(1)–O(1)	88.80(6)	O(1)–Mn(1)–N(1)	163.17(7)
O(4)–Mn(1)–N(2)	86.06(6)	N(2)–Mn(1)–N(1)	72.20(6)
O(2)–Mn(1)–N(2)	162.44(7)		

D–H$\cdots$A	d(D–H)	d(H$\cdots$A)	d(D$\cdots$A)	<(DHA)
O(1)–H(1B)$\cdots$O(2)#1	0.84(2)	2.43(2)	2.987(2)	125(2)
O(1)–H(1B)$\cdots$O(3)#3	0.84(2)	2.25(2)	3.047(2)	158(3)
O(1)–H(1C)$\cdots$O(6)	0.79(2)	1.95(2)	2.742(2)	178(3)
O(6)–H(6A)$\cdots$O(4)	0.85(2)	2.56(3)	3.129(3)	125(2)
O(6)–H(6A)$\cdots$O(5)	0.85(2)	1.93(2)	2.770(3)	174(3)
O(6)–H(6B)$\cdots$O(5)#4	0.86(2)	1.91(2)	2.767(3)	175(3)

Symmetry transformations used to generate equivalent atoms:

#1 $-x + 2, -y + 1, z - 1/2$; #2 $-x + 2, -y + 1, z + 1/2$; #3 $x, y, z - 1$; #4 $-x + 2, -y + 2, z - 1/2$

and 2.2763(18) Å. The bond angles around the metal center range from 72.20(6) to 168.25(7). These values are analogous to those found on similar Mn(II) compounds [22, 23]. In complex **1**, a 1D zig-zag chain is formed due to the combined monodentate and bridging monodentate (to two metal centers), coordination modes of mal (Fig. 2). Hydrogen-bonding interactions in complex **1** are promoted by the presence of the lattice water molecule and the non-coordinated oxygen atom of the mal carboxylate. This is shown in Fig. 3, where the O–H$\cdots$O interactions involve the lattice water molecule (O6) with each oxygen atom (O5) of the non-coordinated side of one mal ligand, in an intramolecular hydrogen bond. Furthermore, each lattice water molecule (O6) generates a double hydrogen bridge; the one described above, and another with an oxygen atom (O5) of the non-coordinated side of mal ligand belonging to a neighboring 1D polymeric chain (intermolecular hydrogen bonding). In this way, an extended 2D supramolecular array is generated (Fig. 3).

Crystal Structure of 2

In the crystal structure of **2**, two [Ni(H$_2$O)$_3$(C$_{12}$H$_{12}$N$_2$)(C$_4$H$_2$O$_4$)] complex molecules are associated into a dinuclear complex throughout hydrogen bonds formed by the O4 of the non-coordinated carboxylate of mal and O5 and O6 of aqua ligands (Fig. 4). In this uncommon dinuclear complex formed by supramolecular interactions, each metal center is six-coordinated and surrounded by three coordinated water molecules, two nitrogen atoms from a 4dmb and one oxygen atom from a maleate ligand, yielding thus distorted octahedral coordination geometry. The Ni–O distances are between 2.0468(12) and 2.0904(14) Å, and the Ni-N distances are 2.0598(14) and 2.0583(14). The bond angles around the metal center range from 79.87(6) to 176.88(5). These values are comparable to those found on similar Ni(II) compounds [24, 25]. These high Z' structures indicate high energy minima in the crystallization path towards the final thermodynamic crystal. Sometimes the process leading to the formation of these crystals is referred to as "frozen" or interrupted crystallization [3]. In comparison to those structures where the kinetic and thermodynamic forms are the same, complexes having asymmetrical units with more than one molecule ($Z' > 1$) are still considered as rarities in crystallography, since crystal structures with these characteristics are relatively small in number [3, 26]. Furthermore, hydrogen-bonding interactions assemble complex **2** into a 2D supramolecular array with 1D rods of two-row Ni centers joint by lattice water molecules (Fig. 5). These intramolecular and

Table 3 Selected bond distances (Å), angles (°) and hydrogen bonding for **2**

Bond lengths (Å)			
Ni(1)–O(1)	2.0468(12)	Ni(1)–O(7)	2.0768(13)
Ni(1)–N(2)	2.0583(14)	Ni(1)–O(6)	2.0904(14)
Ni(1)–N(1)	2.0598(14)		
Ni(1)–O(5)	2.0611(14)		

Angles (°)			
O(1)–Ni(1)–N(2)	98.00(5)	N(1)–Ni(1)–O(7)	95.38(6)
O(1)–Ni(1)–N(1)	175.36(5)	O(5)–Ni(1)–O(7)	89.51(5)
N(2)–Ni(1)–N(1)	79.87(6)	O(1)–Ni(1)–O(6)	90.90(5)
O(1)–Ni(1)–O(5)	88.95(5)	N(2)–Ni(1)–O(6)	88.13(5)
N(2)–Ni(1)–O(5)	88.80(5)	N(1)–Ni(1)–O(6)	93.14(5)
N(1)–Ni(1)–O(5)	86.89(5)	O(5)–Ni(1)–O(6)	176.88(5)
O(1)–Ni(1)–O(7)	86.63(5)	O(7)–Ni(1)–O(6)	93.59(5)
N(2)–Ni(1)–O(7)	175.04(5)		

D–H⋯A	d(D–H)	d(H⋯A)	d(D⋯A)	<(DHA)
O(5)–H(5B)⋯O(4)#1	0.841(15)	2.033(16)	2.8360(18)	160(2)
O(5)–H(5A)⋯O(8)#2	0.841(14)	1.870(14)	2.709(2)	175.4(19)
O(6)–H(6B)⋯O(2)	0.852(14)	1.907(15)	2.734(2)	163(2)
O(6)–H(6A)⋯O(4)#3	0.827(14)	1.882(15)	2.7014(17)	170.5(19)
O(7)–H(7B)⋯O(4)	0.824(14)	2.125(15)	2.9489(19)	179(2)
O(7)–H(7A)⋯O(3)#3	0.844(14)	1.890(14)	2.7297(19)	173.4(19)
O(8)–H(8B)⋯O(3)#4	0.840(15)	2.139(16)	2.971(2)	171(2)
O(8)–H(8A)⋯O(2)	0.841(15)	1.879(16)	2.701(2)	165(2)
O(9)–H(9A)⋯O(3)#5	0.850(12)	2.114(10)	2.9579(19)	172(2)

Symmetry transformations used to generate equivalent atoms:

#1 − x + 3/2, y + 1/2, − z + 3/2; #2 x, y + 1, z; #3 − x + 3/2, y − 1/2, − z + 3/2; #4 x, y − 1, z #5 x + 1/2, y − 1/2, z

**Table 4** Selected bond distances (Å), angles (°) and hydrogen bonding for **3**

Bond lengths (Å)			
Cu(1)–O(3)	1.9230(12)	Cu(1)–N(1)	1.9927(14)
Cu(1)–O(1)	1.9497(12)	Cu(1)–O(1)#1	2.3834(11)
Cu(1)–N(2)	1.9815(13)		

Angles (°)			
O(3)–Cu(1)–O(1)	91.89(5)	N(2)–Cu(1)–N(1)	81.63(5)
O(3)–Cu(1)–N(2)	91.30(5)	O(3)–Cu(1)–O(1)#1	94.47(5)
O(1)–Cu(1)–N(2)	174.00(5)	O(1)–Cu(1)–O(1)#1	79.75(5)
O(3)–Cu(1)–N(1)	171.72(5)	N(2)–Cu(1)–O(1)#1	105.07(5)
O(1)–Cu(1)–N(1)	94.79(5)	N(1)–Cu(1)–O(1)#1	91.54(5)

D–H⋯A	d(D–H)	d(H⋯A)	d(D⋯A)	<(DHA)
O(5)–H(5B)⋯O(2)#2	0.836(16)	1.933(16)	2.7595(19)	170(3)
O(5)–H(5A)⋯O(4)	0.823(16)	2.012(16)	2.821(2)	168(3)
O(6)–H(6A)⋯O(5)#3	0.860(13)	1.913(13)	2.771(3)	175(3)
O(6)–H(6B)⋯O(7)	0.829(19)	1.967(18)	2.786(3)	169(4)
O(7)–H(7A)⋯O(4)#4	0.873(17)	1.986(18)	2.852(3)	172(3)
O(7)–H(7C)⋯O(6)	0.852(19)	1.955(19)	2.786(3)	165(4)

Symmetry transformations used to generate equivalent atoms:

#1 − x + 3/2, − y + 3/2, − z + 1; #2 − x + 3/2, y − 1/2, − z + 3/2; #3 − x + 1, y, − z + 3/2; #4 x − 1/2, y + 1/2, z

**Fig. 1** Molecular structure of **1** (ellipsoids shown at 50% probability)
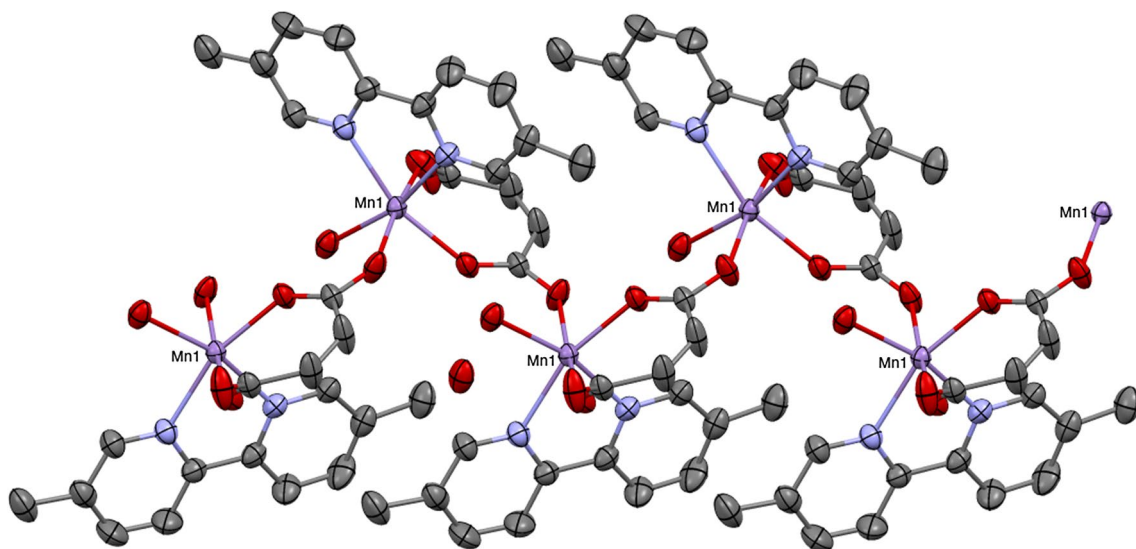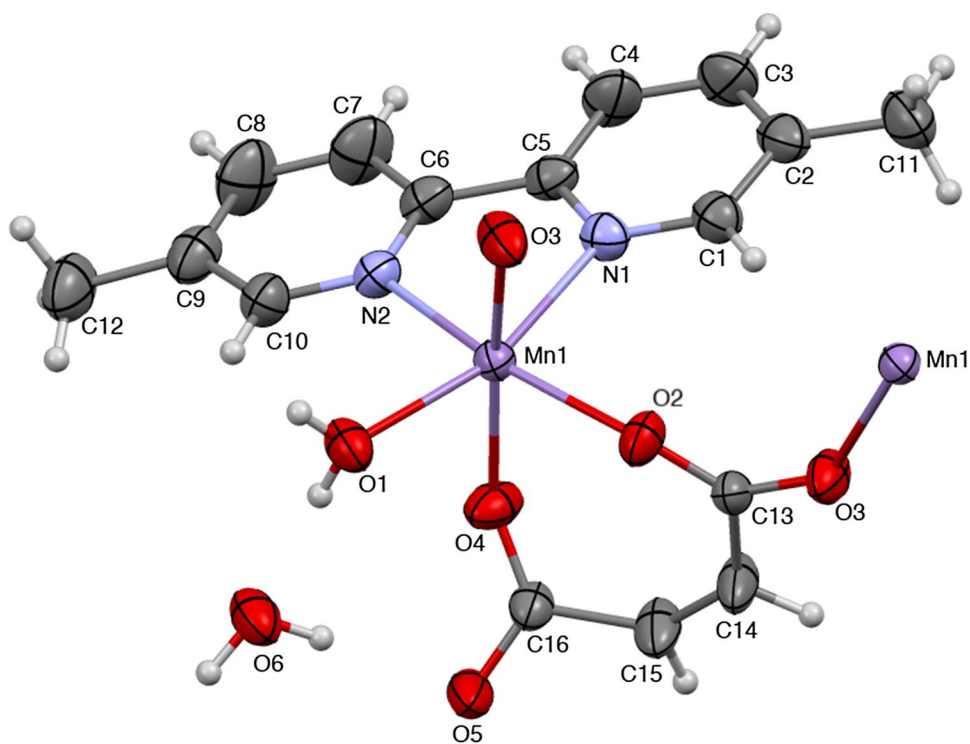
Fig. 2 1D zig-zag polymer chain of **1**; hydrogen atoms omitted for clarity

intermolecular assemblies are motivated by the presence of the three molecules of water in the crystal, and their interactions with the aqua ligands and coordinated and non-coordinated oxygen atoms of the mal ligand (Table 3). In addition, π–π interactions, with a distance of 3.725 Å, occur in the crystal structure of **2** due to the presence of the bipyridine ligands.

Crystal Structure of 3

3 Crystallizes in a monoclinic system with a C2/c space group. A unique Cu(II) dinuclear complex is formed when two mal ligands bind, with one oxygen atom (O1) each, to two different Cu ions (μ$_2$-oxo), forming a rhombic cluster made of two Cu ions and two oxygen atoms (Fig. 6). The angles O1–Cu-O1 = 79.75° and Cu1–O1–Cu1 = 100.25°
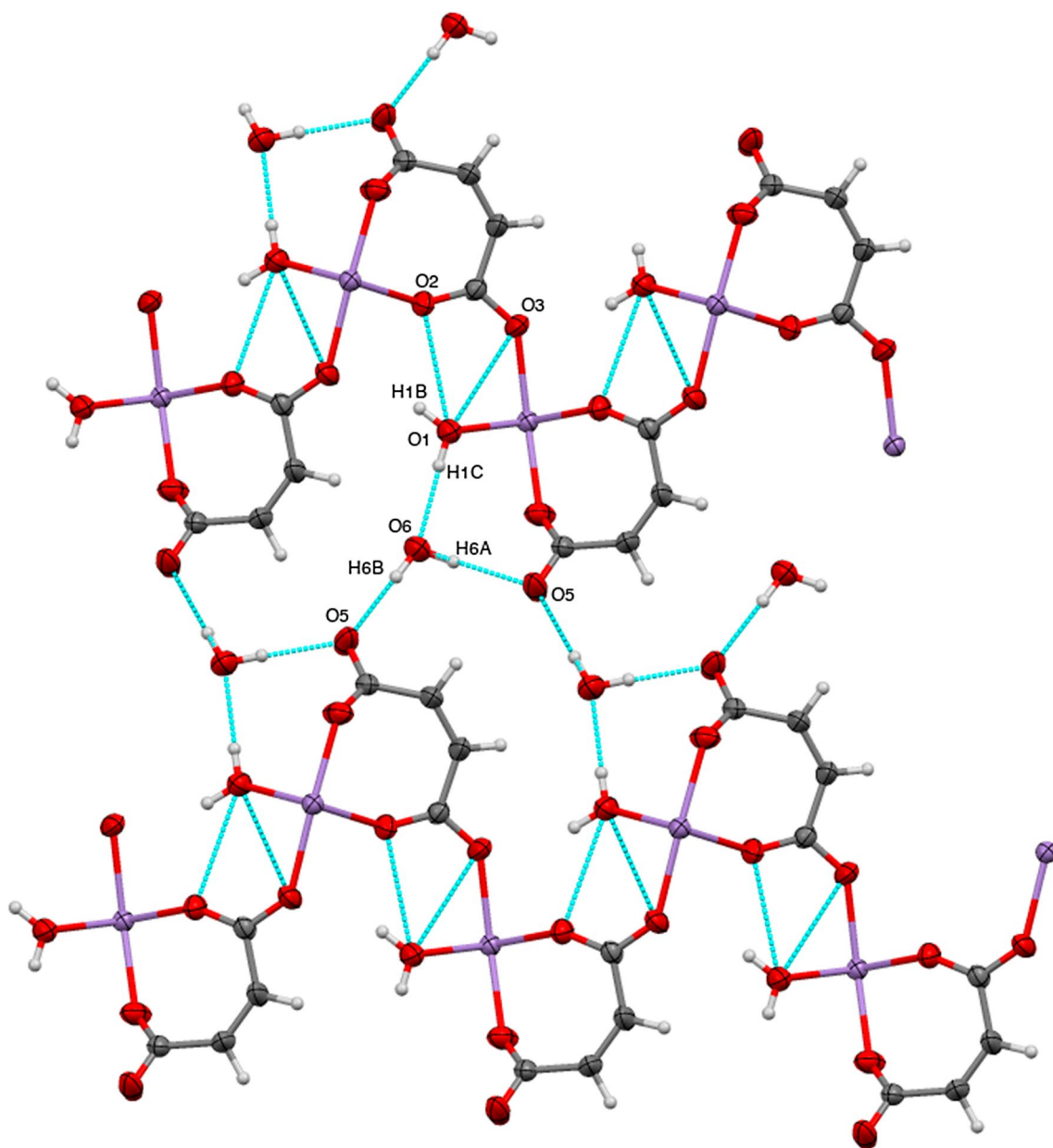
Fig. 3 2D supramolecular array in **1**; 5dmb ligand omitted for clarity

corroborate the rhombic and, since this compound is centrosymmetric, a planar (dihedral angle of 0.0°) geometry of the dimer. The distance between Cu···Cu ions is 3.33 Å, which is larger than those found for paddle-wheel type compounds (2.58–2.65 Å) [27], although it is closer to those originated in complexes having bridging Cu–O–Cu square dimeric clusters (3.05–3.12 Å) [28, 29]. The two Cu centers are doubly bridged by the O atoms of the two chelating-bridging maleates (Fig. 6). Relatively few coordination complexes, or polymers, have been reported showing this type of Cu_2O_2 rhombic cluster [29–34]. The Cu centers are five-coordinated and surrounded by three oxygen atoms from two

mal ligands and two nitrogen atoms from one 4dmb ligand. The metal center displays a slightly distorted square pyramidal configuration (Fig. 6). In this coordination geometry, the basal plane is defined by O1, O3, N1 and N2, from the mal and 4dmb ligands, respectively. The apical position is occupied by O1, from one mal carboxylate. Towards the apical ligating atom, the metal ion is deviated from the corresponding basal plane just by 0.082 Å. The basal plane is found to be barely tetrahedral distorted, with a τ value of 0.038 [τ = (174.01–171.72)/60 = 0.038] (Fig. 6). This τ parameter describes the different coordination geometries in penta-coordinated complexes: $\tau = 0$ for square pyramidal and $\tau = 1$
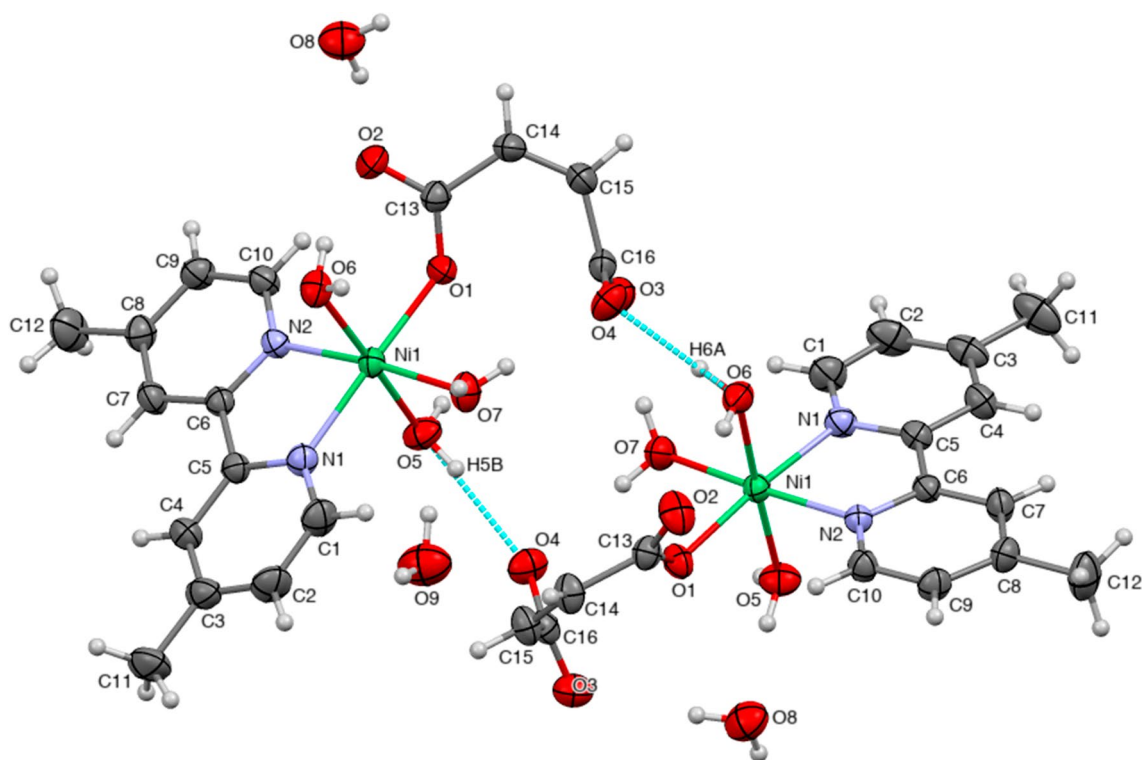
Fig. 4 Molecular structure of **2** (symmetry operation: $1.5 - x$, $0.5 + y$, $1.5 - z$; ellipsoids shown at 50% probability)

for trigonal bipyramidal [24]. The Cu–O bond lengths range from 1.9230(12) to 2.3834(11) Å, while the Cu–N distances are 1.9814(13) and 1.9926(14) Å; these values are similar to those found on comparable Cu(II) compounds [29–31]. Hydrogen bond interactions gather complex **3** into a 3D supramolecular array (Fig. 7). These bindings are formed by the presence of three molecules of water in the crystal, and their contacts with the non-coordinated oxygen atoms of the mal ligand (Table 4). Moreover, due to the presence of the bipyridine moieties there are π–π interactions, with distances of 3.574 and 3.860 Å, in the crystal structure of **3**.

Conclusion

We have reported the synthesis and crystalline molecular and supramolecular structures of three novel complexes of Mn(II), Ni(II) and Cu(II), **1**–**3**, respectively, employing maleato and dimethyl-2,2′-bipyridines as ligands. **1** is a 1D polymer, where the Mn centers are six-coordinated in a distorted octahedral geometry. **2** is a dinuclear complex, generated by supramolecular interactions, where Ni ions are six-coordinated in a distorted octahedral geometry. **3** is a dinuclear complex with five-coordinated Cu ions

having a slightly-distorted square pyramidal geometry. Furthermore, solid-state assemblies on the structures of **1**–**3** generate supramolecular frameworks, mainly through hydrogen bonding: 2D for complexes **1** and **2**, and 3D for complex **3**. Thus, the versatility in the different coordination modes of maleato ligand: chelate bidentate and bridging-monodentate for polymer **1**, monodentate for complex **2** and chelate bidentate for complex **3**; has been evidenced by generating divergent coordination compounds of three different transition metals using facile self-assembly reactions.
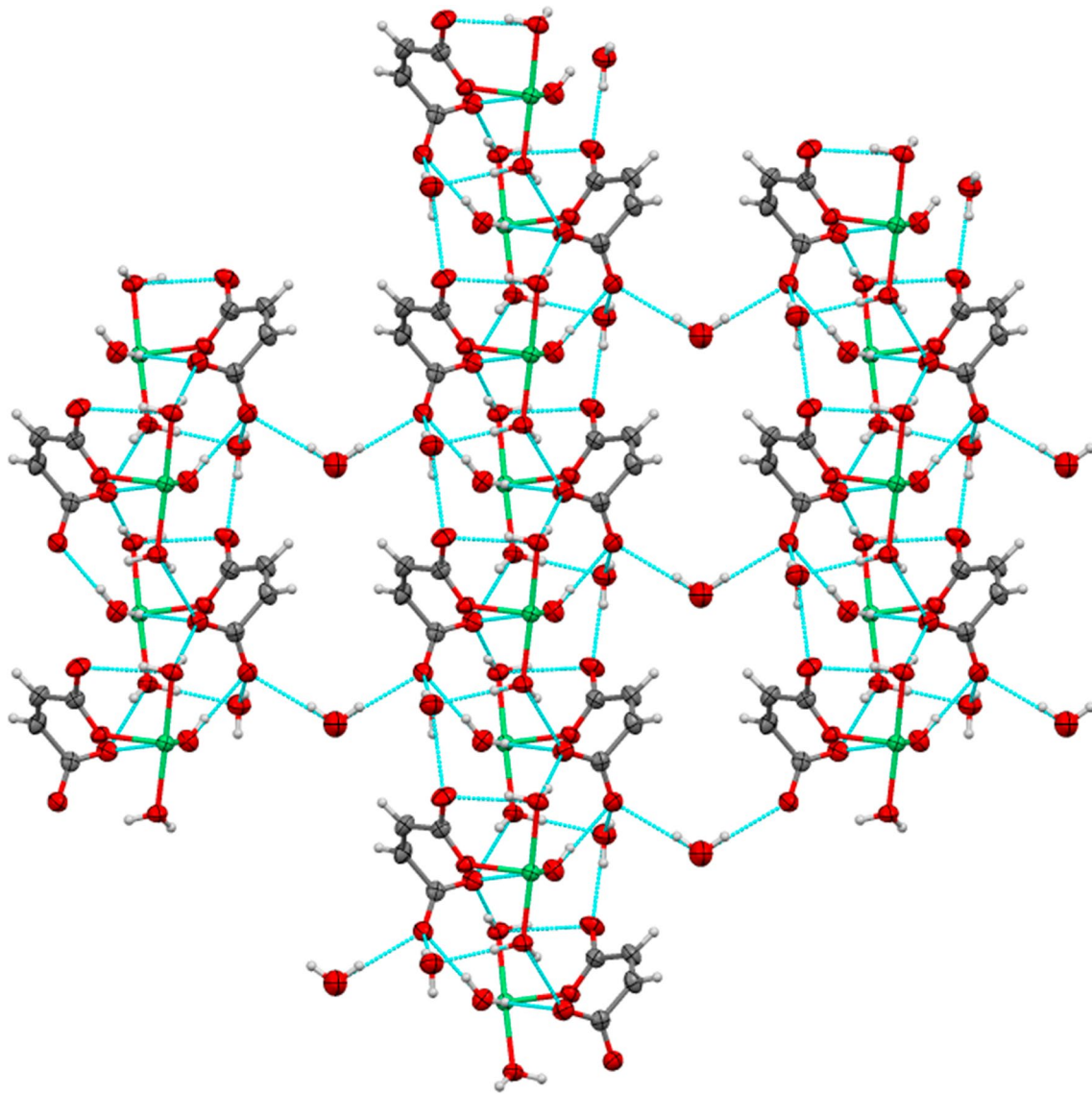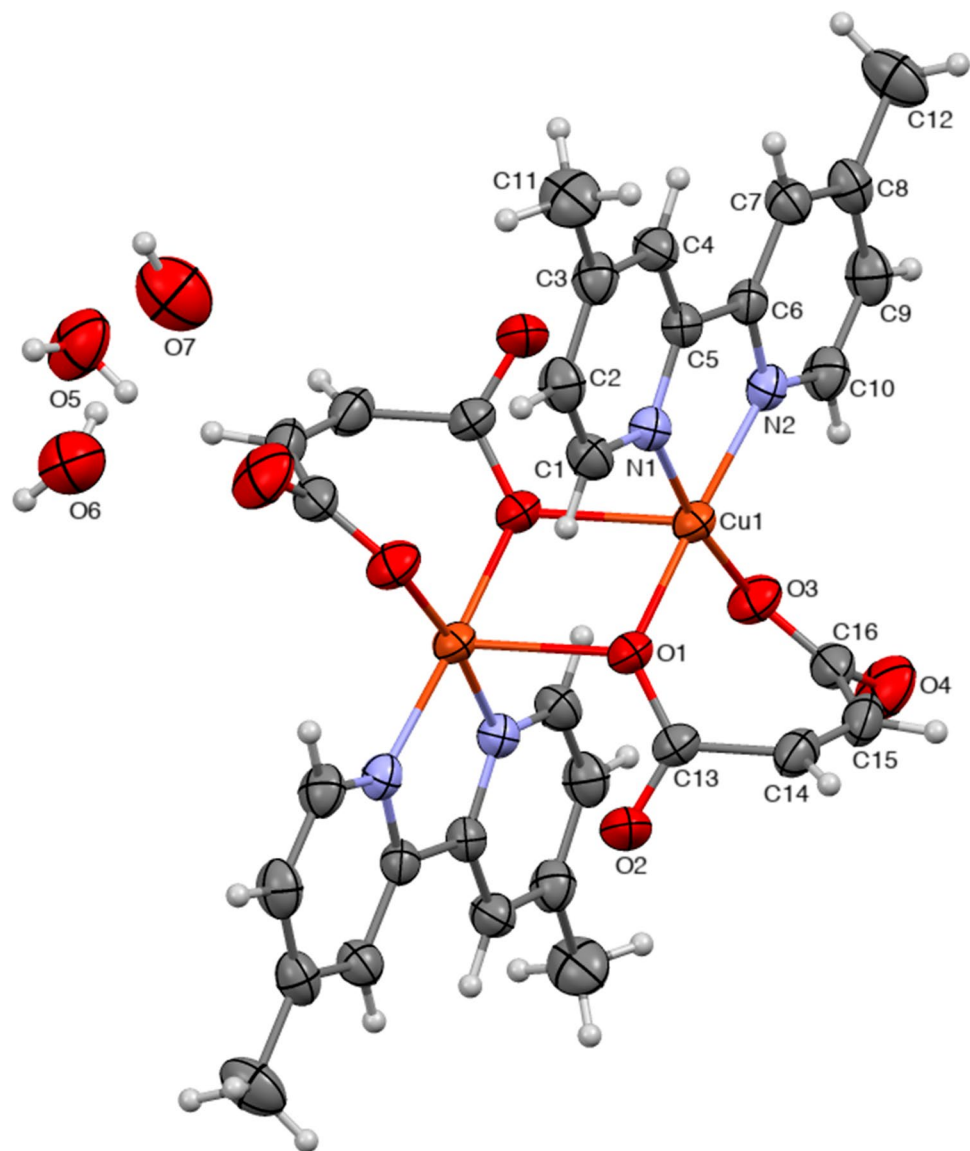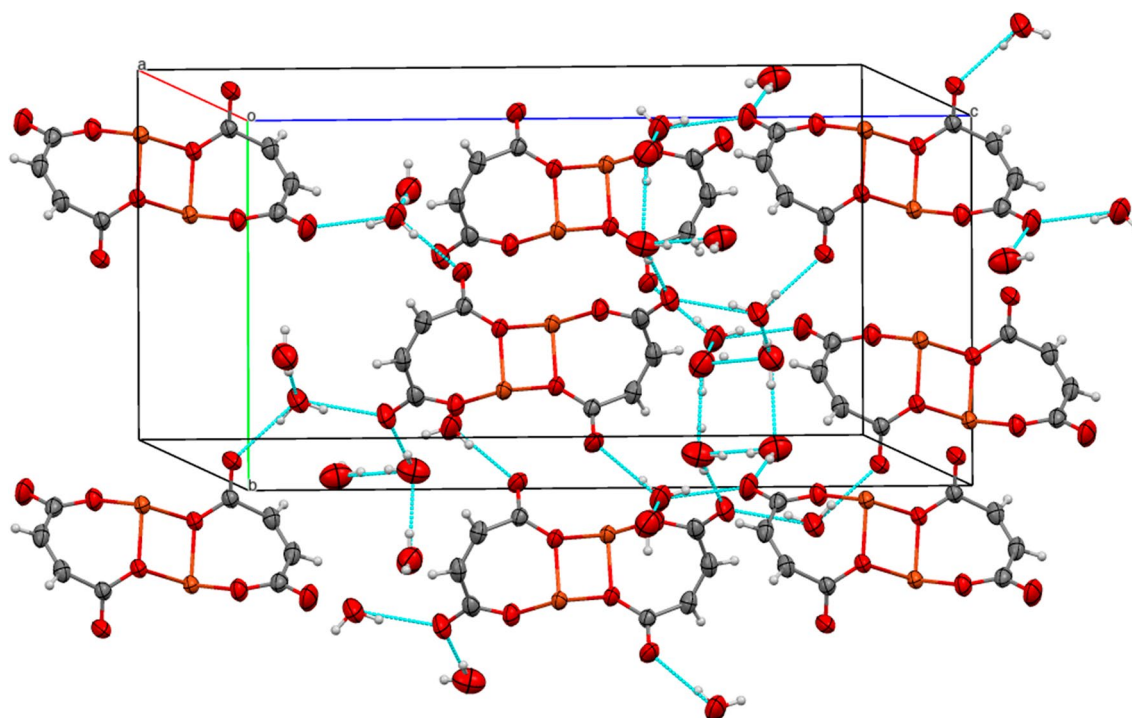
Supplementary Data

Fig. 5 2D supramolecular array in **2**; looking down *ab* plane. 4dmb ligand omitted for clarity

Fig. 6 Molecular structure of **3** (ellipsoids shown at 50% probability)

Fig. 7 3D supramolecular array in **3**; hydrogen atoms and 4dmb ligand omitted for clarity

Compliance with Ethical Standards

Conflict of interest The authors declare that they have no conflict of interest.

References

1. Zhou HC, Long JR, Yaghi OM (2012) Chem Rev 112:673
2. Dua M, Li CP, Liub CS, Fang SM (2013) Coord Chem Rev 257:1282
3. Das D, Banerjee R, Mondal R,. Howard JAK, Boese R, Desiraju GR (2006) Chem Commun 555
4. Zhou XH, Li L, Li HH, Li A, Yang T, Huang W (2013) Dalton Trans 42:12403
5. Lusby PJ (2013) Annu Rep Prog Chem A 109:254
6. Lescop C (2017) Acc Chem Res 50(4):885
7. Ye BH, Tong ML, Chen XM (2005) Coord Chem Rev 249:545
8. Curiel D, Más-Montoya M, Sánchez G (2014) Coord Chem Rev 284:19
9. Rosales-Vázquez LD, Sánchez-Mendieta V, Dorazco-González A, Martínez-Otero D, García-Orozco I, Morales-Luckie RA, Jaramillo-García J, Téllez-López A (2017) Dalton Trans 46:12516
10. Téllez-López A, Jaramillo-García J, Martínez-Domínguez R, Morales-Luckie RA, Camacho-López MA, Escudero R, Sánchez-Mendieta V (2015) Polyhedron 100:373
11. Téllez-López A, Sánchez-Mendieta V, Jaramillo-García J, Rosales-Vázquez LD, García-Orozco I, Morales-Luckie RA, Escudero R, Morales-Leal F (2016) Trans Met Chem 41:879
12. Zhao RL, Yue KF, Zhou C, Cheng QDM, Shi JT, Liu YL, Wanga YY (2013) Inorg Chim Acta 402:25
13. Farnum GA, Martin DP, Sposato LK, Supkowski RM, LaDuca RL (2010) Inorg Chim Acta 363:250
14. Hancock RD (2013) Chem Soc Rev 42:1500
15. Alizadeh R, Amani V (2016) Inorg Chim Acta 443:151
16. Lopes LB, Corrêa CC, Guedes GP, Vaz MGF, Diniz R, Machado FC (2013) Polyhedron 50:16
17. Zhang GM, Li Y, Zou XZ, Zhang JA, Gu JZ, Kirillov AM (2016) Trans Met Chem 41:153
18. APEX 2 Software Suite. Bruker AXS Inc., Madison
19. Sheldrick GM (2008) Acta Crystallogr A 64:112
20. Hübschle CB, Sheldrick GM, Dittrich B, shelXle (2011) Appl Cryst 44:1281
21. Macrae CF, Bruno IJ, Chisholm JA, Edgington PR, McCabe P, Pidcock E, Rodriguez-Monge L, Taylor R, van de Streek J, Wood PA (2008) Mercury CSD 2.0-New features for the visualization and investigation of crystal structures. J Appl Cryst 41:466
22. Rodríguez-Martín Y, Hernández-Molina M, Delgado FS, Pasán J, Ruiz-Pérez C, Sanchiz J, Lloret F, Julve M (2002) Cryst Eng Comm 4(87):522
23. Rodríguez-Martín Y, Hernández-Molina M, Delgado FS, Pasán J, Ruiz-Pérez C, Sanchiz J, Lloret F, Julve M (2003) Dalton Trans 11:2359
24. Ruiz-Pérez C, Hernández-Molina M, Sanchiz J, López T, Lloret F, Julve M (2000) Inorg Chim Acta 298:245
25. Jiang CH, Qi YM, Sun Y, Chi Q, Guo YM (2012) J Mol Struct 1017:65
26. Choudhury SR, Lee HM, Hsiao TH, Colacio E, Jana AD, Mukhopadhyay S (2010) J Mol Struct 967:131

27. Addison AW, Rao TN, Reedijk J, van Rijn J, Verschoor GC (1984) J Chem Soc Dalton Trans 1349
28. Youngme S, Cheansirisomboon A, Danvirutai C, Pakawatchai C, Chaichit N (2008) Inorg Chem Commun 11:57
29. Tokii T, Watanabe N, Nakashima M, Muto Y, Morooka M, Ohba S, Saito Y (1990) Bull Chem Soc Jpn 63:364
30. Boonmak J, Youngme S, Chotkhun T, Engkagul C, Chaichit N, van Albada GA, Reedijk J (2008) Inorg Chem Commun 11:1231
31. Nath JK, Mondal A, Powell AK, Baruah JB (2014) Cryst Growth Des 14:4735
32. Das K, Panda U, Datta A, Roy S, Mondal S, Massera C, Askun T, Celikboyun P, Garribba E, Sinha C, Anand K, Akitsu T, Kobayashi K (2015) New J Chem 39:7309
33. Novoa N, Roisnel T, Dorcet V, Cador O, Manzur C, Carrillo D, Hamon JR (2016) New J Chem 40:5920
34. Mahapatra P, Ghosh S, Giri S, Rane V, Kadam R, Drew MGB, Ghosh A (2017) Inorg Chem 56:5105